Geophysical Research Letters

RESEARCH LETTER
10.1029/2024GL110735

Key Points:

- The estimated LES/CRM entrainment rates increase with increasing resolution, and the growth rate is roughly power-law related to resolution
- The majority of entrainment schemes fail to reproduce the monotonic increase in entrainment rate with increasing resolution
- Entrainment scaling helps reduce the parcel buoyancy and thus the convective available potential energy toward higher resolutions

Supporting Information:

Supporting Information may be found in the online version of this article.

Correspondence to:

X. Wang,
wangxc@lasg.iap.ac.cn

Citation:

Zhao, Y., Wang, X., Liu, Y., & Wu, G. (2024). Are parameterized entrainment rates as scale-dependent as those estimated from cloud resolving model simulations? *Geophysical Research Letters*, *51*, e2024GL110735. https://doi.org/10.1029/2024GL110735

Received 17 JUN 2024
Accepted 11 SEP 2024

Author Contribution:

Conceptualization: Xiaocong Wang
Supervision: Xiaocong Wang
Writing – review & editing: Xiaocong Wang

Are Parameterized Entrainment Rates as Scale-Dependent as Those Estimated From Cloud Resolving Model Simulations?

Yaxin Zhao[1,2], Xiaocong Wang[3], Yimin Liu[1,2], and Guoxiong Wu[2,3]

[1]Key Laboratory of Earth System Numerical Modeling and Application, Institute of Atmospheric Physics, Chinese Academy of Sciences, Beijing, China, [2]College of Earth and Planetary Sciences, University of Chinese Academy of Sciences (UCAS), Beijing, China, [3]State Key Laboratory of Numerical Modeling for Atmospheric Sciences and Geophysical Fluid Dynamics (LASG), Institute of Atmospheric Physics (IAP), Chinese Academy of Sciences (CAS), Beijing, China

Abstract Entrainment rates at varying horizontal grid spacing were diagnosed and analyzed based on Large Eddy Model (LES) and Cloud Resolving Model (CRM) simulations of shallow and deep convection. Results show the estimated entrainment rates increase with increasing resolution, and the growth rate is roughly power-law related to resolution. However, all commonly used parameterizations except for the buoyancy sorting scheme fail to reproduce the monotonic increase of entrainment with resolution, but rather a slight decrease instead. For these schemes, it is suggested the power-law fitting formula derived from LES/CRM simulations can be used as a scaling function for high-resolution entrainment correction. Preliminary tests show that the application of entrainment scaling largely reduces the parcel buoyancy and thus the convective available potential energy, favoring the reduction of parameterized convection at high resolution.

Plain Language Summary As model resolution continues to increase with increasing computational power, cumulus convection becomes partially resolved by the model grid, which requires parameterized convection to be reduced with increasing resolution. The purpose of this study is to investigate the scale dependence of entrainment rate, which is an important component in convection parameterization, by using multiple cloud resolving model simulations of shallow and deep convections. It was found that the estimated entrainment rates increase with increasing resolution, but most current entrainment schemes are unable to reproduce the monotonic increase in entrainment rate with increasing resolution. As a result, a scaling factor between entrainment and resolution was derived and suggested for use in correcting parameterized entrainment rates at high resolution.

1. Introduction

Cumulus convection is key to the energy and hydrological cycle of the Earth system, transporting heat, moisture, and momentum via convective eddy, often parameterized by the use of a mass flux formulation (A. Arakawa & Schubert, 1974; Yanai et al., 1973; Yano, 2014). Typically, a convective scheme consists of a closure assumption that determines the strength of convection, and an entraining plume model that determines the property of a convective parcel. In the plume model, the mixing between convective parcels and their surrounding environment, usually measured in terms of an entrainment rate, plays a crucial role in determining the buoyancy excess and hence the height of the convective plume (C. S. Bretherton & Park, 2008; de Rooy et al., 2013). Numerous entrainment parameterizations have been proposed in the literature, such as those based on the buoyancy sorting concept (Bretherton et al., 2004; de Rooy & Siebesma, 2008; Kain & Fritsch, 1990; Raymond & Blyth, 1986), those based on the neutral buoyancy concept (A. Arakawa & Schubert, 1974; G. J. Zhang & McFarlane, 1995), and those using relative humidity as a predictor (Bechtold et al., 2008). While these schemes have had some success in climate modeling, they need to be scrutinized when applied to high-resolution models, as they were developed primarily for coarse-resolution models. On the other hand, observational analyses have identified the basic features of entrainment rate at high resolution. For example, Romps (2010) and Dawe and Austin (2011) found from large eddy model simulations that entrainment rate increases with decreasing distance from the edge of the cloud core, which was subsequently confirmed by Lu et al. (2012) from aircraft observations. The scale dependence of entrainment rate would become more prominent as the resolution continues to increase. It is worth exploring whether current entrainment schemes can realistically reproduce the scale dependence of entrainment rate as in reality.

It is well known that parameterized convection must be appropriately reduced with increasing resolution so as to ensure that subgrid convective eddy transport reduces to zero when the convective flow is explicitly resolved. This is usually achieved by scaling the mass flux using the convective fraction (A. Arakawa & Wu, 2013). While sufficient attention has been paid to the problem of the closure assumption in high-resolution modeling (Ahn & Kang, 2018; A. Arakawa & Wu, 2013; Plant & Craig, 2008; Sakradzija et al., 2016), little progress has been made in validating and improving the scale dependence of entrainment rate. The purpose of this study is to quantify the relationship between the entrainment rate and the horizontal scales using large eddy model (LES) and cloud resolving model (CRM) simulations of shallow and deep convection, and to answer the question of whether current entrainment schemes can realistically reproduce this scale awareness. As shown in the paper, most schemes are unable to reproduce the monotonic increase of entrainment rate with increasing resolution. Therefore, a scaling function between entrainment rate and horizontal scale is derived from LES/CRM simulations and suggested for use in correcting parameterized entrainment rates at high resolutions.

2. Data and Method

2.1. Shallow and Deep Convection Cases

For both shallow and deep convection, two cases are selected for each type of convection, all coming from the Global Energy and Water Cycle Experiment (GEWEX) Cloud System Studies (GCSS) Working Group on boundary layer and deep convection clouds. The two shallow convection cases are the Barbados Oceanographic and Meteorological Experiment (BOMEX) (Gu et al., 2020; Siebesma et al., 2003), and Rain in Cumulus over the Ocean (RICO) (Vanzanten et al., 2011). The two deep convection cases are the Tropical Rainfall Measuring Mission (TRMM) Kwajalein Experiment (KWAJEX) (Schumacher et al., 2008; Wang & Zhang, 2015) and the Global Atmospheric Research Program's Atlantic Tropical Experiment (GATE) (Wang & Zhang, 2013; Xie & Zhang, 2000). These four cases span a variety of cumulus convection occurring in the tropics.

2.2. Model and Experiments

We choose the model of System for Atmospheric Modeling (SAM) developed by Khairoutdinov and Randall (2003) for LES/CRM modeling. The dynamical framework of SAM is based on the anelastic equations of motion, and the model solves prognostic equations for the three components of velocity and the thermodynamic variables. The model configuration is the same as Zhao, Wang, Liu, Wu & Liu (2024). For BOMEX, the model uses a horizontal resolution of 64×64 with a grid spacing of 100 m and a vertical resolution of 75 levels from the surface to 3,000 m. For RICO, the vertical dimension is extended to 100 levels according to the GCSS specification. For these two shallow convection cases, precipitation process is turned off to guarantee that total moisture is exactly conserved during model integration. For KWAJEX and GATE, the model was set up with 64 levels in the vertical, which gradually increases from 75 m at the surface to a spacing of 400 m through the troposphere and a larger spacing of 1 km in the Newtonian damping region near the model top. The horizontal domain is 256×256 with a grid spacing of 1 km. The large-scale forcing to drive the model is based on the constrained variational approach of M. H. Zhang & Lin (1997) and Zhang et al. (2001). The model is integrated for 6 hr for BOMEX, 24 hr for RICO, 52.25 days for KWAJEX, and 20 days for GATE. The three-dimensional variables are saved every 3 s for shallow convection for the last hour, and every 6 min for deep convection for two consecutive days toward the end of the runs.

2.3. Diagnosis of Entrainment Rate

Following A. Siebesma & Cuijpers (1995), we estimate entrainment rates using a standard bulk plume method that diagnoses entrainment rates from the convective flux of some conserved tracer. Assuming horizontal homogeneity within a plume and the surrounding environment (i.e., top hat approximation), the diagnosis of the fractional entrainment rate ε is expressed as

$$\varepsilon = \frac{\frac{\partial \phi_c}{\partial t}}{w_c(\phi_e - \phi_c)} + \frac{\overline{\overrightarrow{\nabla_h} \cdot \left(\phi \rho \overrightarrow{V_h} \mathcal{A}\right)} - \overline{\phi_c \overrightarrow{\nabla_h} \cdot \left(\rho \overrightarrow{V_h} \mathcal{A}\right)}}{\overline{\rho} a_c w_c (\phi_e - \phi_c)} + \frac{\frac{\partial \phi_c}{\partial z}}{\phi_e - \phi_c} \quad (1)$$

Detailed derivations following Romps (2010) are omitted but provided in Text S1 in Supporting Information S1. In Equation 1, the subscript c denotes active cloudy part, that is, grid points with condensate (larger than 1×10^{-5} kg/kg) and upward vertical velocity, and e the surrounding environment. The overbar represents the horizontal average, and $\mathcal{A}$ is the active operator that is 1 in cloud portion and 0 in environment. Variables ρ, a_c, w_c represent air density, convective fraction, and in-cloud vertical velocity, respectively. The conserved variable ϕ we choose is the total water for shallow convection and the moist static energy for deep convection, although the latter is only approximately conserved due to precipitation (Romps, 2010). The first two terms on the right-hand side of Equation 1 arise from local changes, and changes in lateral boundary fluxes influenced by advective process. With respect to the full domain, the second term vanishes due to the doubly period boundary condition in the LES/CRM. By averaging samples over longer time periods, for example, 10 min for shallow convection, and 1 hr for deep convection, the plume can be approximated as being in a steady state. In addition, the changes due to advective processes largely compensate each other over longer time periods. To a crude approximation, the diagnosis of the entrainment rate ε is simplified to Equation 2, where only the third term is retained.

$$\varepsilon = \frac{\frac{\partial \phi_c}{\partial z}}{\phi_e - \phi_c} \tag{2}$$

Equation 2 is the same as that used by Wang and Zhang (2014) and Eissner et al. (2021), where entrainment rate is determined solely by the dilution of convective properties, in agreement with the cumulus governing formulations in entraining bulk plume models. While the top-hat approximation in coarse resolution models has been justified (A. Siebesma and Cuijpers, 1995), its soundness in high resolution models has not been validated and should be used with caution. It is also worth noting that there are other methods for estimating entrainment rates in the literature (e.g., Jeevanjee & Zhou, 2022; Lu et al., 2012). To derive the entrainment rate at different length scales, we apply the coarse-graining approach that was widely used in previous studies (e.g., Dorrestijn et al., 2013; Honnert et al., 2011; Huang et al., 2018). Specifically, we divide the original LES/CRM domain with area $L \times L$ into subdomains of the same size of $l \times l$ to represent the GCM grid cell. In each subdomain, Equation 2 is applied to calculate the entrainment rate, which is then averaged over all K ($K = \left(\frac{L}{l}\right)^2$) subdomains to yield the average entrainment rate for the corresponding resolution. For both shallow and deep convection, the length scale l decreases consecutively by a factor of 2 from the full domain size to twice the grid spacing 2δx, equivalent to an increase in resolution from 1× to $\frac{L}{2\delta x}$×. For the rest of this paper, the length scale and resolution will be used interchangeably.

3. Results and Analysis

3.1. Scale Dependence of Entrainment Rate in LES/CRM Simulations

Before examining the entrainment rate, we first show in Figures 1a and 1c the profiles of the environmental property ϕ_e at different resolutions. As noticed, ϕ_e increases gradually with increasing resolution almost throughout the entire column. The reason for this is that as the resolution increases, some subdomains that were originally part of the low-resolution active cloudy category now belong to the environment category, so the ambient air within each subdomain gets closer to the cumulus core, which is usually warmer and more humid. The increase in the environmental property is more evident in Figures 1b and 1d (dashed lines), which show the environmental properties at cloud base and the middle portion of the cloud. Given that the active cloudy property ϕ_c does not experience appreciable changes with resolution (solid lines), increasing ϕ_e with increasing resolution implies that the entrainment rate ε should also increase as long as the denominator in Equation 2 dominates the dependence on resolution.

Figure 2 shows the entrainment rate ε estimated from LES/CRM simulations at different resolutions. For shallow convection, we find ε generally increases with increasing resolution from 1× (64 km × 64 km) to 32× (2 km × 2 km) for almost every layer. As mentioned before, this is because the denominator in Equation 2 decreases with increasing resolution while the numerator exhibits little variation. Essentially this is because as the resolution increases, the entrained air becomes closer to the air inside the humid shell around the cumulus core (Lu et al., 2012), thus reducing the difference against the active cloudy portion (shadings in Figures 1b and 1d). The entrainment rate increases almost twofold when the resolution is increased from 1× to 32×. For deep convection,

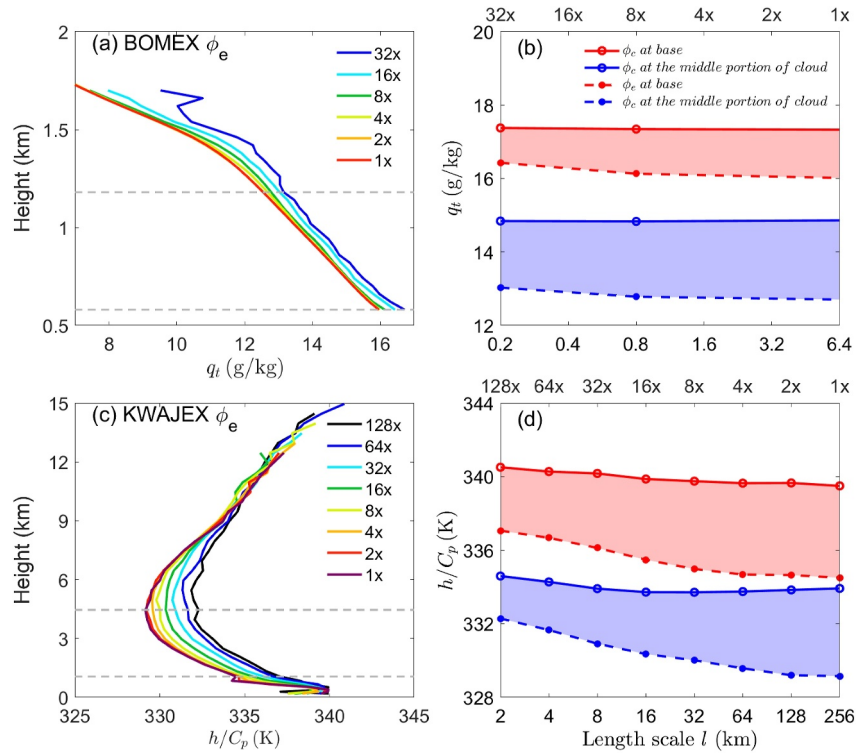

Figure 1. Vertical profiles of environmental property ϕ_e for (a) BOMEX and (c) KWAJEX with varying horizontal resolution. In-cloud property ϕ_c (solid) and environmental property ϕ_e (dashed) at cloud base and cloud middle for (b) BOMEX and (d) KWAJEX. The two Gy lines in (a) and (c) indicate cloud base and cloud middle, respectively.

the entrainment rate ε at 1× resolution (i.e., 256 km × 256 km) is about 0.1 km^{-1}and generally decreases with increasing height, the magnitude of which is in line with many previous studies (Böing et al., 2012; Guo et al., 2015; Zhang et al., 2016). Similar to those seen in shallow convection, ε gradually increases with increasing resolution throughout the troposphere, reaching an order of magnitude of 1 km^{-1} when the resolution is increased to 128× (i.e., 2 km × 2 km).

3.2. Validating Scale-Dependence of Parameterized Entrainment Rates

To see whether current entrainment parameterizations can capture the scale-dependence of entrainment rate seen in LES/CRM simulations, we investigate the performance of three widely-used entrainment schemes, including the buoyancy sorting scheme (BS scheme hereafter) for shallow convection (Bretherton et al., 2004), the neutral buoyancy scheme (ZM scheme hereafter) for deep convection (G. J. Zhang & McFarlane, 1995), and the relative humidity based scheme (RH-based scheme hereafter) for both shallow and deep convections (Bechtold et al., 2008). Details of these schemes are provided in Text S2 in Supporting Information S1. For each scheme, the parameterized entrainment at different horizontal resolutions is calculated based on the grid-scale variables of subdomains obtained by the coarse-graining method.

Figures 3a and 3b show the variation of parameterized entrainment rates with resolution for the BOMEX case. It can be seen that the parameterized ε from the BS scheme increases with increasing resolution, in agreement with the results of LES simulations, although the value of ε is too small at coarse resolution and the growth rate is too large at high resolution compared to LES simulations. On the other hand, the RH-based scheme shows the opposite result, where the parameterized ε decreases with resolution instead. The RH-based scheme assumes that the higher relative humidity is favorable for convection, and therefore ε needs to be reduced to attain a higher cumulus top. On the other hand, the BS scheme argues that a larger ε is needed to dilute convective parcels for achieving neutral buoyancy in an environment with higher relative humidity. That the relative humidity typically increases with increasing resolution in convection-occurring grids (Figure S1 in Supporting Information S1) explains why parameterized ε increases with resolution in the BS scheme and decreases with resolution in the RH-

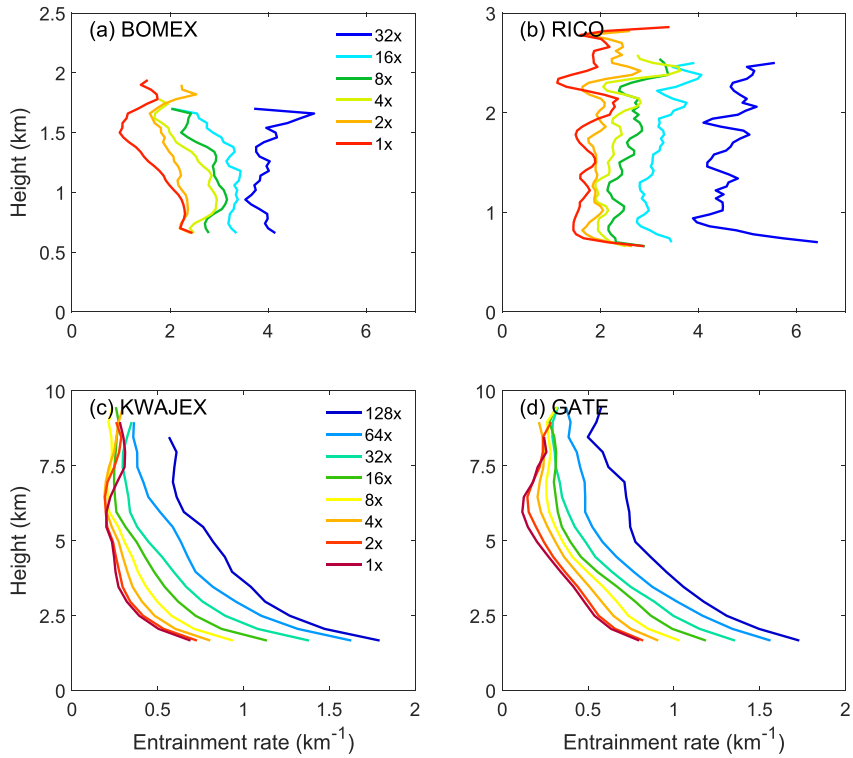

Figure 2. Vertical profiles of entrainment rate estimated from LES/CRM at different horizontal resolution for (a) BOMEX, (b) RICO, (c) KWAJEX, and (d) GATE.

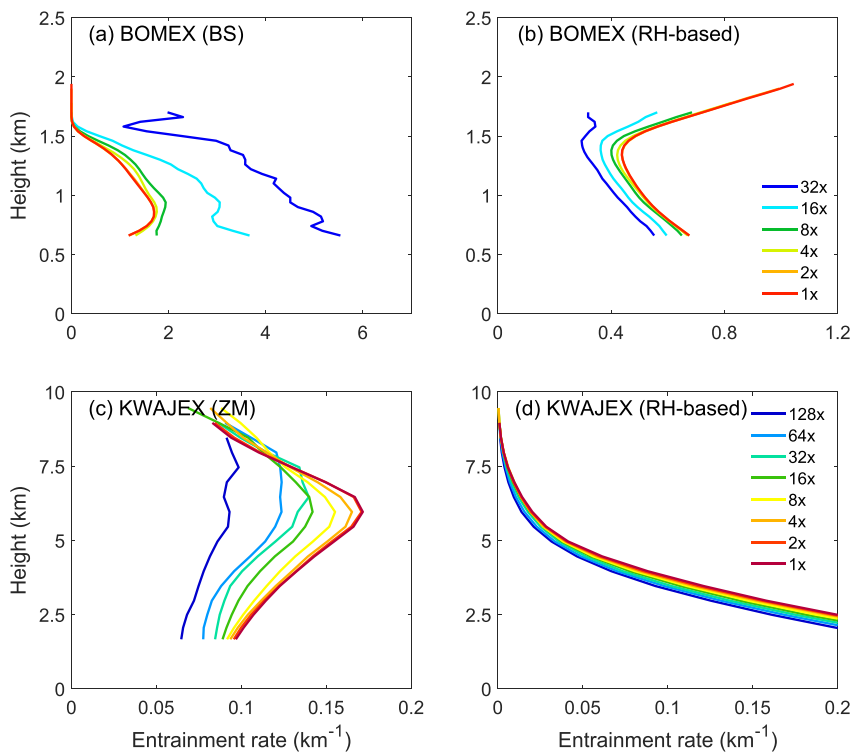

Figure 3. Parameterized entrainment rate at different horizontal resolution for BOMEX by (a) the buoyancy sorting (BS) scheme, and (b) the RH-based scheme. Parameterized entrainment rate for KWAJEX by (c) the neutral buoyancy (ZM) scheme, and (d) the RH-based scheme.

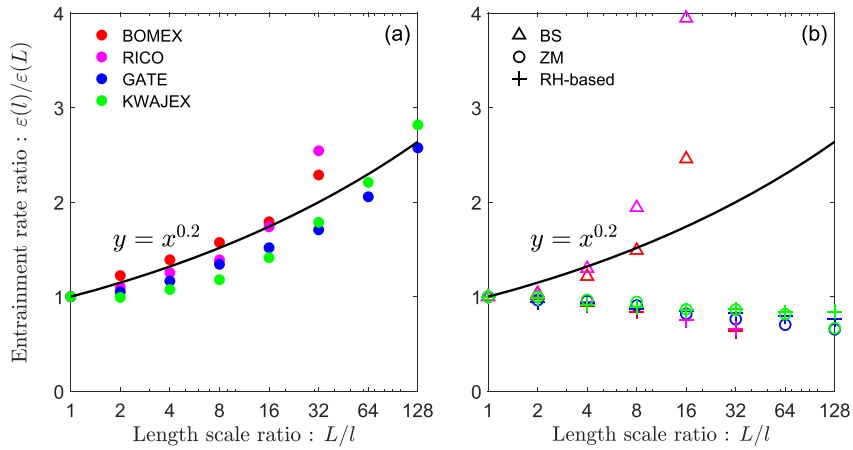

Figure 4. Scatterplots of entrainment scale ratio ($\varepsilon(l)/\varepsilon(L)$) versus length scale ratio (L/l) for all four convection cases: (a) estimated from LES/CRM simulations, and (b) parameterized by different entrainment schemes. Each point represents a vertical mean of $\frac{\varepsilon(l)}{\varepsilon(L)}$ for each case and the black line indicates the best-fit curve for LES/CRM results.

based scheme. Figures 3c and 3d show the variation of entrainment rate with resolution for the KWAJEX case calculated from the ZM scheme and the RH-based scheme, respectively. Similar to BOMEX, the parameterized ε according to the RH-based scheme decreases with increasing resolution. In contrast to the BS scheme, the parameterized ε by the ZM scheme decreases with increasing resolution. However, this should not come as a surprise even though both schemes use buoyancy as a predictor. This is because in the ZM scheme, it is not only the difference in moist static energy inside and outside of the cloud that affects entrainment rate, but also the vertical height of the cumulus cloud (Text S2 in Supporting Information S1). In other words, the ZM scheme can dilute the buoyancy by raising the height of cumulus top, in addition to increasing the entrainment rate. In terms of the relationship between entrainment and resolution, the ZM scheme operates similarly to the RH-based scheme, but opposite to the BS scheme and CRM simulations. Similar features were also found in the RICO and GATE cases (Figure S2 in Supporting Information S1), further validating the assertion drawn above.

3.3. Scaling Function Between Entrainment Rate and Horizontal Resolution

To quantify how the LES-estimated entrainment rate varies with resolution, Figure 4a shows the scatterplot of the entrainment rate ratio defined as $\frac{\varepsilon(l)}{\varepsilon(L)}$ on the ordinate, versus the length scale ratio defined as $\frac{L}{l}$ on the abscissa, for all four cases. Each point represents a vertical mean of $\frac{\varepsilon(l)}{\varepsilon(L)}$ for each case. It is worth noting here that we are concerned with the ratio of entrainment rate, not the entrainment rate per se. It can be seen that the ratio of entrainment rate increases monotonically with the length scale ratio, with the points generally collapsing on a power-law curve denoted as $y = x^{0.2}$. In addition to the oceanic convective cases shown here, the ratio of entrainment rate in the continental convective case also obeys a power-law relationship (Figure S3 in Supporting Information S1). A caveat is that only one LES/CRM model was used and the reported results may suffer from model uncertainties (Jeevanjee & Zhou, 2022; Jenny et al., 2023). It is also worth noting that varying the entrainment rate in parameterized scheme can affect the background state, which in turn affects the entrainment rate per se (Kuo et al., 2017). All parameterizations except for the BS scheme shown in Figure 4b fail to reproduce the monotonic increase of the entrainment rate ratio with the increase of length scale ratio, but rather a slight decrease instead. While the BS scheme performs well in the resolution range of 2× to 8×, beyond 8× it grossly overestimates the growth rate of entrainment rate.

Since entrainment parameterization such as in the ZM and the RH-based schemes do not experience significant changes with resolution, the fitting formula derived from LES/CRM simulations can be used as a scaling factor to correct the relationship between ε and resolution in entrainment schemes. To understand the impact of this scaling factor on convective parameterization, we apply it to a plume model (Text S3 in Supporting Information S1) equipped with the RH-based scheme and show in Figure 5 the parcel buoyancy and convective available potential energy (CAPE) at different resolutions for the KWAJEX case. Large-scale fields such as moist stability and

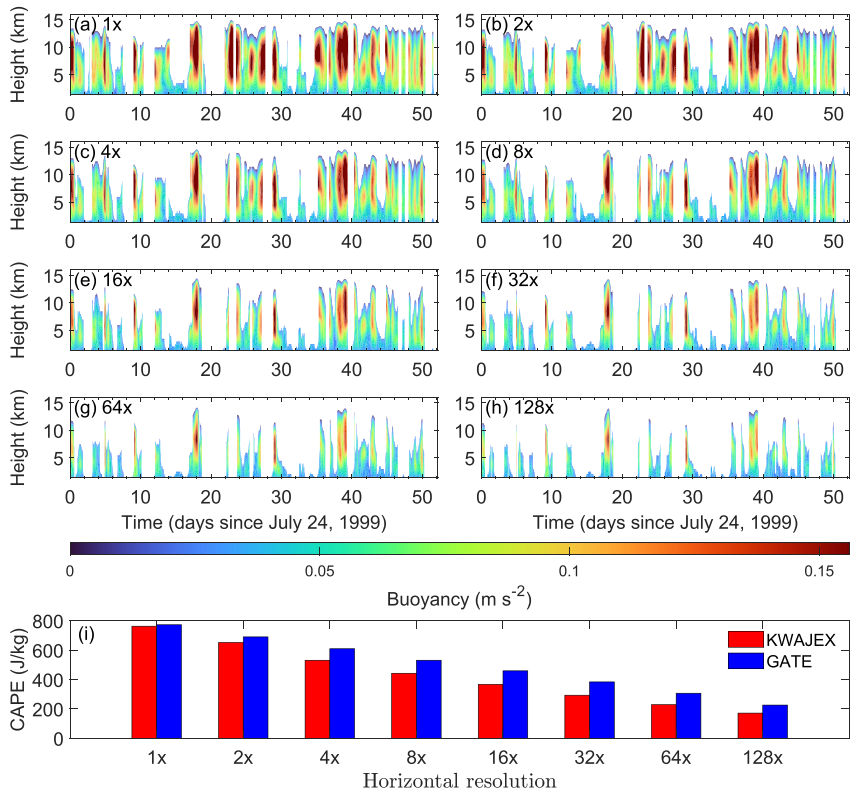

Figure 5. Simulated buoyancy profile of KWAJEX in a bulk plume model after applying the scaling factor to the RH-based entrainment scheme at resolution of (a) 1×, (b) 2×, (c) 4×, (d) 8×, (e) 16×, (f) 32×, (g) 64×, and (h) 128×. (i) Convective available potential energy calculated at different resolution for both KWAJEX and GATE.

relative humidity, which are inputs to the entraining plume model, are assumed to be the same as those at the 1× resolution, which approximately holds true in the tropics as fast gravity waves can keep the temperature of the column the same as that of the surrounding environment (Emanuel & Sobel, 2013), that is, the weak-temperature gradient (WTG) approximation. Figures 5a–5h shows a remarkable drop in the buoyancy profile from the resolution of 1× to 128×, with the latter having only one-fifth the magnitude of the former. In addition, cumulus clouds become shallower at higher resolution, especially in a weakly unstable atmosphere. Similar phenomena were also found in the GATE case (Figure S4 in Supporting Information S1). The decrease in buoyancy, together with the shallowing of cumulus height results in CAPE decreasing remarkably with increasing resolution as shown in Figure 5i. The calculated CAPE at the resolution of 128× is about a quarter of the CAPE at the resolution of 1×. Thus, in addition to adjusting cumulus mass flux, the scaling of entrainment rate could potentially provide another way to help the convective parameterization achieve scale-awareness, further ensuring that subgrid convective transport drops to zero in the limit of convection resolving.

4. Conclusion and Discussion

In this study, the entrainment rate at different horizontal scale is diagnosed from LES/CRM simulations of shallow and deep convection using a coarse-graining approach, using soundings from the BOMEX, RICO, KWAJEX and GATE campaigns. Results show that the entrainment rate increases with increasing resolution in both shallow and deep convections, due to the fact that the difference in properties between the active cloud portion and the surrounding environment tends to decrease with resolution. Essentially, this is caused by the increase in the environmental humidity, which gradually gets closer to the cumulus core as resolution increases. The dependence of the entrainment on resolution roughly satisfies a power law relationship denoted as $y = x^{0.2}$. This empirical scaling should be used with caution as only one LES/CRM model was used and the results may be model dependent.

To see whether current entrainment schemes can realistically capture the scale-dependence of entrainment rate as in LES/CRM simulations, three widely used entrainment parameterizations are investigated, including the BS scheme, the ZM scheme, and the RH-based scheme. All parameterizations except for the BS scheme fail to reproduce the monotonic increase of the entrainment rate with resolution, but rather a slight decrease instead. For entrainment schemes that are not scale aware, it is recommended that the fitting formula derived from LES/CRM simulations can be used as a scaling factor to correct entrainment rates at high resolution. Applying the scaling factor to the RH-based scheme results in remarkable reduction in the parcel buoyancy and shallower cumulus top height, leading to CAPE only one-fifth that of the original scheme. Therefore, in addition to closure, the scaling of entrainment could potentially provide another effective way to help convective parameterization achieve scale-awareness, further ensuring that subgrid convective eddy transport is reduced to zero when the convective flow is explicitly resolved at high resolution.

Data Availability Statement

All LES/CRM datasets used in this study are available at https://doi.org/10.5281/zenodo.11739325 (Zhao, Wang, Liu, & Wu, 2024).

Acknowledgments
We thank the two anonymous reviewers whose comments helped improve the original paper. Thanks also go to Marat Khairoutdinov for making his Large-Eddy Simulation model available to us. This work was jointly supported by the National Key R&D Program of China (2021YFC3000802), the National Natural Science Foundation of China (42175165) and the National Key Scientific and Technological Infrastructure project "Earth System Science Numerical Simulator Facility" (EarthLab).

References

Ahn, M.-S., & Kang, I.-S. (2018). A practical approach to scale-adaptive deep convection in a GCM by controlling the cumulus base mass flux. *Npj Climate and Atmospheric Science*, *1*(1), 1–8. https://doi.org/10.1038/s41612-018-0021-0

Arakawa, A., & Schubert, W. (1974). Interaction of a cumulus cloud ensemble with large-scale environment .1. *Journal of the Atmospheric Sciences*, *31*(3), 674–701. https://doi.org/10.1175/1520-0469(1974)031<0674:ioacce>2.0.co;2

Arakawa, A., & Wu, C.-M. (2013). A unified representation of deep moist convection in numerical modeling of the atmosphere. Part I. *Journal of the Atmospheric Sciences*, *70*(7), 1977–1992. https://doi.org/10.1175/JAS-D-12-0330.1

Bechtold, P., Köhler, M., Jung, T., Doblas-Reyes, F., Leutbecher, M., Rodwell, M. J., et al. (2008). Advances in simulating atmospheric variability with the ECMWF model: From synoptic to decadal time-scales. *Quarterly Journal of the Royal Meteorological Society*, *134*(634), 1337–1351. https://doi.org/10.1002/qj.289

Böing, S. J., Siebesma, A. P., Korpershoek, J. D., & Jonker, H. J. J. (2012). Detrainment in deep convection. *Geophysical Research Letters*, *39*(20), L20816. https://doi.org/10.1029/2012GL053735

Bretherton, C. S., McCaa, J. R., & Grenier, H. (2004). A new parameterization for shallow cumulus convection and its application to marine subtropical cloud-topped boundary layers. Part I: Description and 1D results. *Monthly Weather Review*, *132*(4), 864–882. https://doi.org/10.1175/1520-0493(2004)132<0864:ANPFSC>2.0.CO;2

Bretherton, C. S., & Park, S. (2008). A new bulk shallow-cumulus model and implications for penetrative entrainment feedback on updraft buoyancy. *Journal of the Atmospheric Sciences*, *65*(7), 2174–2193. https://doi.org/10.1175/2007JAS2242.1

Dawe, J. T., & Austin, P. H. (2011). Interpolation of LES cloud surfaces for use in direct calculations of entrainment and detrainment. *Monthly Weather Review*, *139*(2), 444–456. https://doi.org/10.1175/2010MWR3473.1

De Rooy, W. C., Bechtold, P., Fröhlich, K., Hohenegger, C., Jonker, H., Mironov, D., et al. (2013). Entrainment and detrainment in cumulus convection: An overview. *Quarterly Journal of the Royal Meteorological Society*, *139*(670), 1–19. https://doi.org/10.1002/qj.1959

De Rooy, W. C., & Siebesma, A. P. (2008). A simple parameterization for detrainment in shallow cumulus. *Monthly Weather Review*, *136*(2), 560–576. https://doi.org/10.1175/2007MWR2201.1

Dorrestijn, J., Crommelin, D. T., Siebesma, A. P., & Jonker, H. J. J. (2013). Stochastic parameterization of shallow cumulus convection estimated from high-resolution model data. *Theoretical and Computational Fluid Dynamics*, *27*(1), 133–148. https://doi.org/10.1007/s00162-012-0281-y

Eissner, J. M., Mechem, D. B., Jensen, M. P., & Giangrande, S. E. (2021). Factors governing cloud growth and entrainment rates in shallow cumulus and cumulus congestus during GoAmazon2014/5. *Journal of Geophysical Research: Atmospheres*, *126*(12), e2021JD034722. https://doi.org/10.1029/2021JD034722

Emanuel, K., & Sobel, A. (2013). Response of tropical sea surface temperature, precipitation, and tropical cyclone-related variables to changes in global and local forcing. *Journal of Advances in Modeling Earth Systems*, *5*(2), 447–458. https://doi.org/10.1002/jame.20032

Gu, J.-F., Plant, R. S., Holloway, C. E., & Muetzelfeldt, M. R. (2020). Pressure drag for shallow cumulus clouds: From thermals to the cloud ensemble. *Geophy. Res. Lett.*, *47*(22), e2020GL090460. https://doi.org/10.1029/2020GL090460

Guo, X., Lu, C., Zhao, T., Zhang, G. J., & Liu, Y. (2015). An observational study of entrainment rate in deep convection. *Atmosphere*, *6*(9), 1362–1376. https://doi.org/10.3390/atmos6091362

Honnert, R., Masson, V., & Couvreux, F. (2011). A diagnostic for evaluating the representation of turbulence in atmospheric models at the kilometric scale. *Journal of the Atmospheric Sciences*, *68*(12), 3112–3131. https://doi.org/10.1175/JAS-D-11-061.1

Huang, W., Bao, J.-W., Zhang, X., & Chen, B. (2018). Comparison of the vertical distributions of cloud properties from idealized extratropical deep convection simulations using various horizontal resolutions. *Monthly Weather Review*, *146*(3), 833–851. https://doi.org/10.1175/MWR-D-17-0162.1

Jeevanjee, N., & Zhou, L. (2022). On the resolution-dependence of anvil cloud fraction and precipitation efficiency in radiative-convective equilibrium. *Journal of Advances in Modeling Earth Systems*, *14*(3), e2021MS002759. https://doi.org/10.1029/2021MS002759

Jenney, A. M., Ferretti, S. L., & Pritchard, M. S. (2023). Vertical resolution impacts explicit simulation of deep convection. *Journal of Advances in Modeling Earth Systems*, *15*(10), e2022MS003444. https://doi.org/10.1029/2022MS003444

Kain, J., & Fritsch, J. (1990). A one-dimensional entraining detraining plume model and its application in convective parameterization. *Journal of the Atmospheric Sciences*, *47*(23), 2784–2802. https://doi.org/10.1175/1520-0469(1990)047<2784:AODEPM>2.0.CO;2

Khairoutdinov, M. F., & Randall, D. A. (2003). Cloud resolving modeling of the ARM summer 1997 IOP: Model formulation, results, uncertainties, and sensitivities. *Journal of the Atmospheric Sciences*, *60*(4), 607–625. https://doi.org/10.1175/1520-0469(2003)060<0607:crmota>2.0.co;2

Kuo, Y.-H., Neelin, J. D., & Mechoso, C. R. (2017). Tropical convective transition statistics and causality in the water vapor–precipitation relation. *Journal of the Atmospheric Sciences*, *74*(3), 915–931. https://doi.org/10.1175/JAS-D-16-0182.1

Lu, C., Liu, Y., Niu, S., & Vogelmann, A. M. (2012). Lateral entrainment rate in shallow cumuli: Dependence on dry air sources and probability density functions. *Geophysical Research Letters*, *39*(20). https://doi.org/10.1029/2012GL053646

Plant, R. S., & Craig, G. C. (2008). A stochastic parameterization for deep convection based on equilibrium statistics. *Journal of the Atmospheric Sciences*, *65*(1), 87–105. https://doi.org/10.1175/2007JAS2263.1

Raymond, D. J., & Blyth, A. M. (1986). A stochastic mixing model for nonprecipitating cumulus clouds. *Journal of the Atmospheric Sciences*, *43*(22), 2708–2718. https://doi.org/10.1175/1520-0469(1986)043<2708:ASMMFN>2.0.CO;2

Romps, D. M. (2010). A direct measure of entrainment. *Journal of the Atmospheric Sciences*, *67*(6), 1908–1927. https://doi.org/10.1175/2010JAS3371.1

Sakradzija, M., Seifert, A., & Dipankar, A. (2016). A stochastic scale-aware parameterization of shallow cumulus convection across the convective gray zone: A stochastic scheme for shallow cumuli. *Journal of Advances in Modeling Earth Systems*, *8*(2), 786–812. https://doi.org/10.1002/2016MS000634

Schumacher, C., Ciesielski, P. E., & Zhang, M. H. (2008). Tropical cloud heating profiles: Analysis from KWAJEX. *Monthly Weather Review*, *136*(11), 4289–4300. https://doi.org/10.1175/2008MWR2275.1

Siebesma, A., & Cuijpers, J. (1995). Evaluation of parametric assumptions for shallow cumulus convection. *Journal of the Atmospheric Sciences*, *52*(6), 650–666. https://doi.org/10.1175/1520-0469(1995)052<0650:eopafs>2.0.co;2

Siebesma, A. P., Bretherton, C. S., Brown, A., Chlond, A., Cuxart, J., Duynkerke, P. G., et al. (2003). A large eddy simulation intercomparison study of shallow cumulus convection. *Journal of the Atmospheric Sciences*, *60*(10), 1201–1219. https://doi.org/10.1175/1520-0469(2003)60<1201:alesis>2.0.co;2

Vanzanten, M. C., Stevens, B., Nuijens, L., Siebesma, A. P., Ackerman, A. S., Burnet, F., et al. (2011). Controls on precipitation and cloudiness in simulations of trade-wind cumulus as observed during RICO. *Journal of Advances in Modeling Earth Systems*, *3*(2), a–n. https://doi.org/10.1029/2011MS000056

Wang, X., & Zhang, M. (2013). An analysis of parameterization interactions and sensitivity of single-column model simulations to convection schemes in CAM4 and CAM5. *Journal of Geophysical Research: Atmospheres*, *118*(16), 8869–8880. https://doi.org/10.1002/jgrd.50690

Wang, X., & Zhang, M. (2014). Vertical velocity in shallow convection for different plume types. *Journal of Advances in Modeling Earth Systems*, *12*(2), 478–489. https://doi.org/10.1002/2014MS000318

Wang, X., & Zhang, M. (2015). The coupling of mixed Rossby-gravity waves with diabatic heating during the TRMM-KWAJEX field campaign. *Geophysical Research Letters*, *42*(19), 8241–8249. https://doi.org/10.1002/2015GL065813

Xie, S., & Zhang, M. (2000). Impact of the convection triggering function on single-column model simulations. *Journal of Geophysical Research*, *105*(D11), 14983–14996. https://doi.org/10.1029/2000JD900170

Yanai, M., Esbensen, S., & Chu, J.-H. (1973). Determination of bulk properties of tropical cloud clusters from large-scale heat and moisture budgets. *Journal of the Atmospheric Sciences*, *30*(4), 611–627. https://doi.org/10.1175/1520-0469(1973)030<0611:DOBPOT>2.0.CO;2

Yano, J.-I. (2014). Basic convective element: Bubble or plume? A historical review. *Atmospheric Chemistry and Physics*, *14*(13), 7019–7030. https://doi.org/10.5194/acp-14-7019-2014

Zhang, G. J., & McFarlane, N. (1995). Sensitivity of climate simulations to the parameterization of cumulus convection in the Canadian climate center general-circulation Model. *Atmosphere-Ocean*, *33*(3), 407–446. https://doi.org/10.1080/07055900.1995.9649539

Zhang, G. J., Wu, X., Zeng, X., & Mitovski, T. (2016). Estimation of convective entrainment properties from a cloud-resolving model simulation during TWP-ICE. *Climate Dynamics*, *47*(7–8), 2177–2192. https://doi.org/10.1007/s00382-015-2957-7

Zhang, M. H., & Lin, J. L. (1997). Constrained variational analysis of sounding data based on column-integrated budgets of mass, heat, moisture, and momentum: Approach and application to ARM measurements. *Journal of the Atmospheric Sciences*, *54*(11), 1503–1524. https://doi.org/10.1175/1520-0469(1997)054<1503:cvaosd>2.0.co;2

Zhang, M. H., Lin, J. L., Cederwall, R. T., Yio, J. J., & Xie, S. C. (2001). Objective analysis of ARM IOP data: Method and sensitivity. *Monthly Weather Review*, *129*(2), 295–311. https://doi.org/10.1175/1520-0493(2001)129<0295:OAOAID>2.0.CO;2

Zhao, Y., Wang, X., Liu, Y., & Wu, G. (2024). Dataset of 4D conserved tracers for convection simulated by large eddy model and cloud resolving model [Dataset]. *Zenodo*. https://doi.org/10.5281/zenodo.11739325

Zhao, Y., Wang, X., Liu, Y., Wu, G., & Liu, Y. (2024). Shallow convection dataset simulated by three different large eddy models. *Advances in Atmospheric Sciences*, *41*(4), 754–766. https://doi.org/10.1007/s00376-023-3106-6